J Solid State Electrochem (2013) 17:1815–1822
DOI 10.1007/s10008-013-2113-4

ORIGINAL PAPER

On electrocatalysis in alkene–molybdenum(VI) system at Pt/acidic solution interface

Maria Bełtowska-Brzezinska · Tomasz Węsierski

Received: 9 December 2012 / Revised: 24 April 2013 / Accepted: 25 April 2013 / Published online: 15 May 2013

Abstract The catalytic reduction of ethene, propene and 1-butene on a polycrystalline Pt electrode in strongly acidic medium containing Mo(VI) oxo-species has been examined by cyclic voltammetry taking into account the influence of perchloric acid and molybdate concentration as well as that of the scan rate on the cathodic current response. About tenfold increase in the reaction rate of each alkene investigated has been achieved at the optimum molybdate concentration of 1–2.5 mM in 4-M $HClO_4$ solution as a supporting electrolyte in comparison with that obtained in the absence of Mo(VI) oxo-species. It was ascertained that the catalytic reduction current strongly depends on the amount of cationic Mo(VI) oxo-species at the Pt electrode/solution interface. Simultaneously, the electroreduction of cationic Mo(VI) oxo-species was found to be effectively enhanced in the presence of alkene. According to the proposed reaction pathways, alkenes are reduced to alkanes via a non-faradaic reaction with Mo(V) and/or Mo(III) cationic moieties formed in the preceding reductive electron-transfer steps from the parent cationic Mo(VI) oxo-species. Continuous regeneration of the electroactive Mo(VI) and/or Mo(V) cationic oxo-species accounts for the observed catalytic phenomenon.

Keywords Electrocatalysis · Electroreduction · Pt/molybdenum(VI)-alkene system

Dedicated to Prof. Dr Wolf Vielstich on the occasion of his 90th birthday

M. Bełtowska-Brzezinska (✉)
Faculty of Chemistry, A. Mickiewicz University, Grunwaldzka 6, 60-780 Poznań, Poland
e-mail: mbb@amu.edu.pl

T. Węsierski
The Main School of Fire Service, Słowackiego 52/54, 01-629 Warszawa, Poland

Introduction

Monitoring of the amount of alkenes in the air is of importance in storage and transport of these hazardous organic compounds in order to avoid fire and/or explosion. In the search for a sensitive electrochemical detection mode we have discovered a substantial enhancement of the reduction rate of ethene, propene and 1-butene on a polycrystalline Pt electrode after addition of Na_2MoO_4 into a strongly acidified solution. Our previous paper [1] has been devoted to the voltammetric behaviour of a propene–Mo(VI) system. The aim of this work is to rationalise the catalytic effect of Mo(VI) oxo-species in electroreduction of ethene and 1-butene at the Pt electrode/solution interface by taking into regard the relevant data obtained for propene under the same experimental conditions. The kinetics of electroreduction of alkenes and molybdate alone on the investigated polycrystalline Pt electrode in acidic solutions is reported for comparison.

Experimental

All studies were conducted in a thermostated (295 K) glass cell, adapted to electrolyte exchange, with three compartments separated by glass frits and equipped with a Luggin capillary in a distance of 2 mm from the working polycrystalline Pt electrode of geometric area of 0.4 cm^2. A hydrogen electrode of Will's type, filled with 1-M $HClO_4$ (NHE) was used as a reference. A large area Pt sheet was a counter electrode. Prior to each experiment the working electrode was activated in the supporting electrolyte solution (deaerated with argon) by cycling (1–10 V/s) between the onset of hydrogen and oxygen evolution until a reproducible voltammogram was obtained. Finally, the roughness factor of Pt ($rf = 2.7 \pm 0.2$) was determined from the charge

corresponding to the hydrogen adsorption-desorption, assuming that a hydrogen monolayer requires 0.21 mC/cm^2.

Cyclic voltammograms (CVs) were obtained in alkene-saturated solutions of perchloric acid without and with Na_2MoO_4 of various concentration as well as after replacement of the reactant-containing electrolyte by a pure supporting electrolyte (electrolyte exchange), following the adsorption of organic species at a constant electrode potential (E_{ad}). Furthermore, potentiodynamic measurements were performed in the supporting electrolyte solutions containing Na_2MoO_4. The potential scan started always at E=0.45 V, at which no faradaic reaction occurs on a Pt electrode in the solutions investigated.

The adsorption experiments were performed according to the following procedure. After a series of eight potentiodynamic scans between 0.07 and 1.65 V, the potential of a working Pt electrode was held at E=1.65 V for 10 ms and then switched (at v=20 V/s) to different fixed E_{ad} values for various time periods, t_{ad}. Next, after electrolyte exchange under potential control, the strongly bonded species remaining at the Pt electrode were oxidised or reduced during the first positive or negative going potential sweep, respectively. We have found that the limiting coverage of the Pt surface with the organic adsorbate was achieved within 300 s for E_{ad} between 0.25 and 0.45 V. This was clearly ascertained by an almost complete suppression of the anodic current related to the hydrogen desorption prior to the beginning of alkene reduction to the respective alkane. It should be emphasised that a reductive removal of the adsorbate from the Pt surface was excluded when the positive going sweep started immediately after switching from E_{ad} to E=0.2 V at v=20 V/s. Therefore, the degree of electrode coverage with alkene species (Θ) was evaluated from the difference ($\Delta Q_{H(0.2–0.4\ V)}$) between the charge related to the oxidative desorption of hydrogen ad-atoms, taking place in the potential range 0.2–0.4 V, on Pt in the supporting electrolyte ($Q^o_{H\ (0.2–0.4\,V)}$) and after adsorption of an individual alkene ($Q_{H(0.2–0.4\ V)}$) at E_{ad}. The following expression was used: $\Theta = \Delta Q_{H(0.2–0.4\,V)}/Q^o_{H(0.2–0.4\,V)}$. In parallel, the charge related to the complete oxidation of alkene adlayers to CO_2 (Q_{ox}) during the first positive going potential sweep was determined by integration of CVs within the potential range E=0.75–1.64 V. The charge corresponding to the oxide layer formation on Pt was subtracted from the total charge determined in the presence of alkenes on the electrode surface. It is worth noting that a typical CV profile of a blank Pt electrode was obtained already during the second positive going potential scan. Finally, the number of electrons transferred per each Pt surface site upon the oxidative desorption of the organic species (n_{eps}) was calculated as: $n_{eps} = Q_{ox}/\Theta \times Q^o_{H,\,total}$ ($Q^o_{H,\,total}$ is the charge corresponding to the hydrogen monolayer on the Pt electrode investigated in the supporting electrolyte).

The apparatus included a computer controlled 9431 potentiostat (Atlas Sollich, Poland) equipped with an IR drop correction system and coupled to a signal generator working in the triangular potential sweep mode, with the programmable potential sequences, potential ranges, number of cycles and scan rates as well as time periods, while holding the electrode potential at a constant value. Current-potential-time dependencies were recorded and analysed with a computer based system connected to a MC112-12 interface (Mescomp, Poland).

Chemicals were used as received (ethene (99.998 %), propene (99.5 %) and 1-butene (99.5 %)) from Linde-Gas, $HClO_4$ suprapur (Merck) and sodium molybdate p.A. grade (Aldrich). Argon (99.998) (BOC-Gas) served for deaeration of the supporting electrolyte solutions with and without Na_2MoO_4, which were made with Millipore-MilliQ water.

Results and discussion

Electroreduction of ethene, propene and 1-butene

Representative current peaks corresponding to irreversible reduction of ethene, propene and 1-butene during the negative going potential scan on a polycrystalline Pt electrode in a 4-M $HClO_4$ solution saturated with these compounds are presented in Fig. 1. Adsorption of each parent compound on the electrode surface, preceding the reductive charge transfer, is clearly manifested by suppression of the current related to the hydrogen adsorption-desorption in the potential range between E=0.4 V and E=0.25 V similarly, as reported for propene on a porous Pt/PTFE electrode [2]. But the following cathodic current peaks at E <0.25 V attributed to the reduction of subsequent alkenes are better developed on the investigated polycrystalline Pt electrode and therefore they are useful for determination of kinetic parameters of these processes.

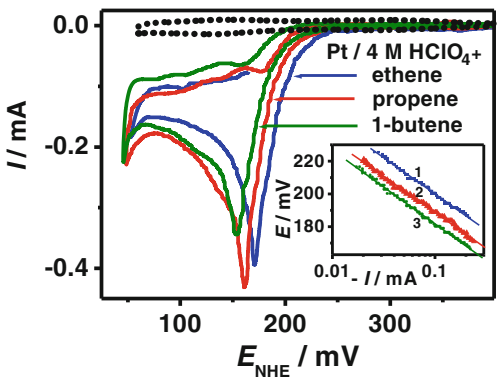

Fig. 1 Fragment of CVs on a polycrystalline Pt electrode in 4-M $HClO_4$ solution saturated with *1* ethene, *2* propene and *3* 1-butene. *Dotted line* CVs on Pt in 4-M $HClO_4$. v = 0.005 V/s. *Insert*: Tafel plot of CVs shown in the main diagram

It is well known from earlier differential electrochemical mass spectrometry (DEMS) studies of propene [2] and ethene [3–8] on Pt/PTFE and single crystal Pt electrodes in sulphuric acid solutions that a large majority of these compounds undergo electroreduction in the hydrogen region to the respective alkanes. This means that the carbon skeleton of the parent compounds remains preserved upon their adsorption and hydrogenation. The dominant adsorbate at E <0.5 V was proved to be the associatively (di–σ and π) bonded ethene and/or propene arranged with the carbon chain almost parallel to the metal surface. Accordingly, the number of electrons released per each Pt site (n_{eps}) and per each carbon atom converted to CO_2 (n_{epm}) upon the complete oxidative desorption of the organic surface species (at E <0.8 V) was found to be close to 6 [2–8]. Almost the same appears to be the nature and orientation of the ad-layer formed on the polycrystalline Pt electrode investigated in this work in perchloric acid solution saturated with ethene, propene or 1-butene. The n_{eps} values elicited from our adsorption experiments ($E_{ad} = 0.25 - 0.45\,V,\ t_{ad} = 300\,s$) with electrolyte exchange were equal to 5.6, 5.75 and 5.7 as predicted for C_2-, C_3- and C_4- alkene molecules lying almost flat at the Pt/solution interface and completely oxidised to CO_2 upon release of 12, 18 and 24 electrons, respectively. In particular, both the maximum electrode coverage with 1-butene species and the anodic current peak with a maximum of about 1.1 V corresponding to their complete oxidative desorption during the first positive going sweep (after a rapid switch from E_{ad} to E=0.2 V) closely resembles those obtained for propene (see Fig. 2). Taking into account that each propene species at Θ≈1 occupy three adjacent Pt sites [2], these experimental data suggest that 1-butene adsorbate consists predominantly of associatively bonded C_4-species spread over four adjacent surface sites of the electrode investigated. Thus, it is reasonable to suppose that the main volatile product of 1-butene electroreduction in the hydrogen region (at E <0.25 V) is butane. Further information is expected from DEMS experiments. However, at the present state of knowledge this assumption is supported by the fact that 100 % conversion of 1-butene and 2-butene to *n*-butane was found in the reaction with hydrogen in the gas phase by using platinum as catalyst at 300–350 K [9]. Most probably, a steric hindrance of the alkyl group prevented the recombination of partially reduced 1-butene species, similarly as has been established for propene [2]. Differently, dimerization of at least a small part of the reduced ethene surface species was ascertained by the evolution of butane besides ethane, albeit in the 1:10 proportion only [3–8].

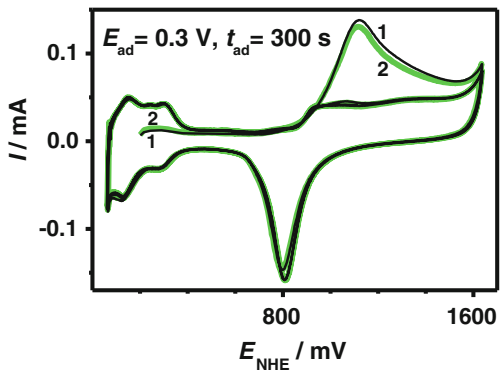

Fig. 2 Voltammetric response of *1* propene and *2* 1-butene species pre-adsorbed on a polycrystalline Pt electrode in 1-M $HClO_4$ at E_{ad}= 0.3 V (t_{ad}=300 s). The first positive going scan (v=0.025 V/s) starts after replacement of the reactant-containing solution with pure supporting electrolyte and switching from E_{ad} to E=0.2 V at 20 V/s

From CVs in Fig. 1, it can be inferred that the reactivity of ethene and 1-butene upon electroreduction at the polycrystalline Pt/solution interface is similar to that found for propene under the same experimental conditions (see also [1]). However, an increase in the carbon chain length in these alkenes results in some shift of the *I-E* dependencies towards lower electrode potentials. A plausible reason for such regularity may be a stronger adsorption of 1-butene, and in consequence, higher activation energy of its reductive desorption than that characteristic of propene and ethene. This is consistent with a general trend of increasing adsorption affinity with a growing number of carbon atoms in the molecule of organic compounds, which was well recognised for various metal electrodes [10–12]. Additionally, the inductive effect of the electron-repelling alkyl group favours charge donation from the π orbitals of the double C=C bond to the vacant orbitals of Pt in passing from ethene to propene and to 1-butene. Moreover, some differences in the reduction rate of individual alkene may be partially caused by increasing steric hindrance in the approach of hydrogen to the surface species with longer carbon chains.

The kinetic data leaves no doubt that each of the alkene under consideration gets reduced according to the same mechanism. Having analysed the CVs, we have established that the half peak potential ($E_{pc/2}$) of ethene and 1-butene electroreduction as well as that of propene [1] takes more positive values by about $dE_{pc/2}/d\log c_{H^+} = 0.06 \pm 0.005$ V at tenfold increase in the acid concentration. Obviously, each electron transfer is accompanied by the addition of one proton to the reduced moieties, as expected on the basis of the general equation: $C_nH_{2n} + 2H^+ + 2e^- \rightarrow C_nH_{2n+2}$. The Tafel slope of $dE/d\log I = 0.045 \pm 0.005$ V/decade, the same for ethene, propene and 1-butene (see insert in Fig. 1), points to the uptake of the second electron and the second hydrogen by the reduced organic species as the rate determining step in the overall reaction pathway at the onset of alkene hydrogenation, i.e., in the initial part of the *I-E* dependencies. However, as follows, from CVs explored at various scan rates (v) and exemplified in Fig. 3 for 1-butene, the rate of the reductive alkene consumption around the potential of the peak maximum up to v≈0.04 V/s exceeds

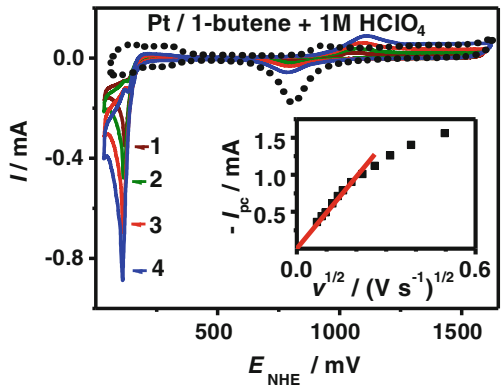

Fig. 3 CVs obtained on a polycrystalline Pt electrode in 1-M $HClO_4$ solution saturated with 1-butene, at various scan rates *v*: *1* 0.005 V/s, *2* 0.01 V/s, *3* 0.02 V/s, *4* 0.035 V/s. *Insert*: dependence of the peak maximum corresponding to the electroreduction of 1-butane on the square root of the scan rate. *Dotted lines* CVs on Pt in 1-M $HClO_4$

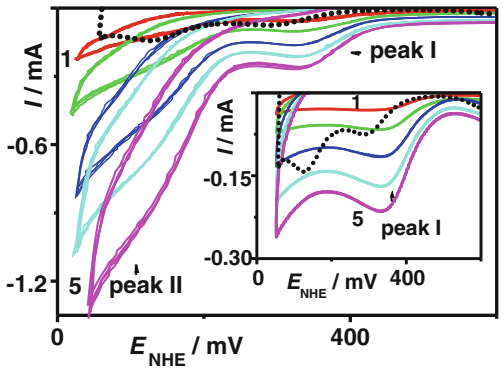

Fig. 4 Fragment of CVs on a polycrystalline Pt electrode in 4-M $HClO_4$+0.5 mM Na_2MoO_4 solution (deaerated with argon) at various scan rates: *1* 0.01 V/s, *2* 0.025 V/s, *3* 0.05 V/s, *4* 0.075 V/s, *5* 0.1 V/s. *Insert* CVs on the same working electrode in 1-M $HClO_4$+0.5 mM Na_2MoO_4, at the same scan rates as in the main diagram. *Dotted lines* CVs on Pt in the supporting electrolyte

that of its adsorption and diffusion from the bulk solution to the Pt electrode. This is reflected in a linear increase in the peak current (I_{pc}) with the square root of *v* (insert in Fig. 3) predicted by the Randles–Ševčik equation for diffusion controlled electrode processes [13]. A negative deviation in the I_{pc}–$v^{1/2}$ plot observed with increasing scan rate suggests that the I_{pc} value at *v* above 0.04 V/s becomes determined by the kinetics of the 1-butene adsorption preceding its hydrogenation. A similar dependence we have found for ethene and also earlier for propene [1]. Nearly equal cathodic currents in the peak maximum related to the electroreduction of the alkene investigated (Fig. 1), being independent of acid concentration, point to an almost the same value of the quotient of the substrate concentration (c_{alkene}) and the square root of the corresponding diffusion coefficient (D_{alkene}) for ethene, propene and 1-butene.

Voltammetric behaviour of Mo(VI) oxo-species

Interestingly, the electroreduction of each individual alkene investigated on a polycrystalline Pt electrode takes place in the potential range close to that of the cathodic peak II (at *E* <0.25 V), which appears on CVs (Fig. 4) obtained in strongly acidified (4 M $HClO_4$) molybdate solutions (without alkene) after the preceding considerably lower cathodic peak I, in the potential range 0.5–0.25 V.

Analysis of the *I-E* dependencies and XPS spectra of the Pt surface described in our previous paper [14] for various concentration of perchloric acid and molybdate ($c_{Mo(VI)} = 0.05-50$ mM), revealed that peak I corresponded to the formation of a mixed-valent Mo(V)/Mo(VI) ad-layer upon electroreduction of pre-adsorbed monomeric molybdic acid in the form of trioxo- and dioxo- moieties ($[Mo^{VI}O_3(H_2O)_3]$, $[Mo^{VI}O_2(OH)_2(H_2O)_2]$) and oligomeric aggregates (from $[Mo^{VI}_{12}O_{40}]^{8-}$ to $[Mo^{VI}_{36}O_{112}]^{8-}$), which predominate in solutions of pH ≥0 [15–19]. As depicted in the insert in Fig. 4, no other electroreduction process of Mo(VI) species can be noticed in the CVs before the hydrogen evolution on Pt in the molybdate solution with 1-M $HClO_4$. The same observation was made for lower perchloric acid concentration. The subsequent current peak II developed in CVs (Fig. 4) after increase in the acid concentration above 1-M $HClO_4$ (at a constant $c_{Mo(VI)}$), has been assigned to the consecutive irreversible electroreduction of singly and doubly charged mononuclear Mo(VI) cationic species [14] being formed favourably at pH <0 (such as $[Mo^{VI}O_2(OH)(H_2O)_3]^+$, $[Mo^{VI}O_2(H_2O)_4]^{2+}$ [15–17]) to the relevant protonated Mo(V)-species ($[Mo^{V}O(OH)_2(H_2O)_3]^+$, $[Mo^{V}O(OH)(H_2O)_4]^{2+}$) and then to Mo(III) cationic moieties ($[Mo^{III}(OH)_2(H_2O)_4]^+$, $[Mo^{III}(OH)(H_2O)_5]^{2+}$). These reactions can be described as:

$$[Mo^{VI}O_2(OH)(H_2O)_3]^+ \xrightarrow{+H^+,+e^-} [Mo^{V}O(OH)_2(H_2O)_3]^+ \xrightarrow{+2H^+,+2e^-} [Mo^{III}(OH)_2(H_2O)_4]^+ \quad (1)$$

$$[Mo^{VI}O_2(H_2O)_4]^{2+} \xrightarrow{+H^+,+e^-} [Mo^{V}O(OH)(H_2O)_4]^{2+} \xrightarrow{+2H^+,2e^-} [Mo^{III}(OH)(H_2O)_5]^{2+} \quad (2)$$

The conclusion that each electron transfer upon reduction of Mo(VI) to Mo(III) cations is accompanied by an addition of one proton to the reduced species, was justified by the shift of the half peak potential ($E_{p/2}$) of cathodic peak II to the positive direction with increasing concentration of H^+ ions in solution by about $E_{p/2}/\log c_{H^+} = 0.06 \pm 0.005$ V at

a tenfold increase in the H^+ concentration in solution. Furthermore, the Tafel slope obtained in the kinetic range of the *I-E* curves, equal to $dE/d\log I = 60 \pm 5$ mV/decade, identified the reduction of Mo(V) to Mo(III) moieties as the rate-determining step.

Because the limiting current of the cathodic peak II attains the greatest magnitude on the Pt electrode in 4-M $HClO_4$ solution with $c_{Mo(VI)} \approx 2.5$ mM [14], there is no doubt that the concentration of electroactive cationic Mo(VI) oxo-species reaches a maximum under such experimental conditions. This is in agreement with the results of UV–vis and Raman spectroscopy studies [15–17]. A gradual decrease in this voltammetric signal at the molybdate concentration above 5 mM suggests a favoured formation of dimeric and/or oligomeric species. On the other hand, the relative distribution of various Mo(VI) forms at the electrode/solution interface remains most probably unaltered upon a successive increase in the H^+ concentration above 4 M, independent of $c_{Mo(VI)}$, as indicated by the absence of any changes in the current response.

Experiments with different scan rates (0.002–0.1 V/s) revealed that the reduction rate of the electroactive cationic Mo(VI) oxo-species in the potential range of the peak (II) is limited by their diffusion from the bulk solution to the electrode surface, whereas the majority of the reduction products, i.e., the respective cationic Mo(V) and/or Mo(III) oxo-species move into the solution [14].

As shown below in Section 3.3, the presence of cationic Mo(VI) oxo-species in the strongly acidified molybdate solutions is a precondition for the catalytic effect found by us in the electroreduction of alkenes.

Catalytic reduction of alkene on a Pt electrode in acidic solutions with cationic Mo(VI) oxo-species

Exemplary CVs in Fig. 5 provide evidence that an addition of Na_2MoO_4 (0.05–5 mM) to a concentrated perchloric acid solution saturated with ethene, propene or 1-butene as well as introduction of each alkene investigated into a strongly acidified molybdate solution bring about an appreciable enhancement of the reduction rate of these compounds on a polycrystalline Pt electrode (at E <0.25 V), in comparison with that characteristic of alkene or molybdate alone in a pure supporting electrolyte of the same concentration.

While the current response (at v=const) related to the electroreduction of alkenes was not influenced by pH of the supporting electrolyte solution without any additive (Fig. 1 and Fig. 3), the extent of catalysis in the presence of molybdate was found to be strongly dependent on the H^+ concentration. Increasing the perchloric acid concentration in solutions containing various constant molybdate concentration ($c_{Mo(VI)}$) and saturated with either ethene, propene or 1-butene we achieved the highest catalytic performance of

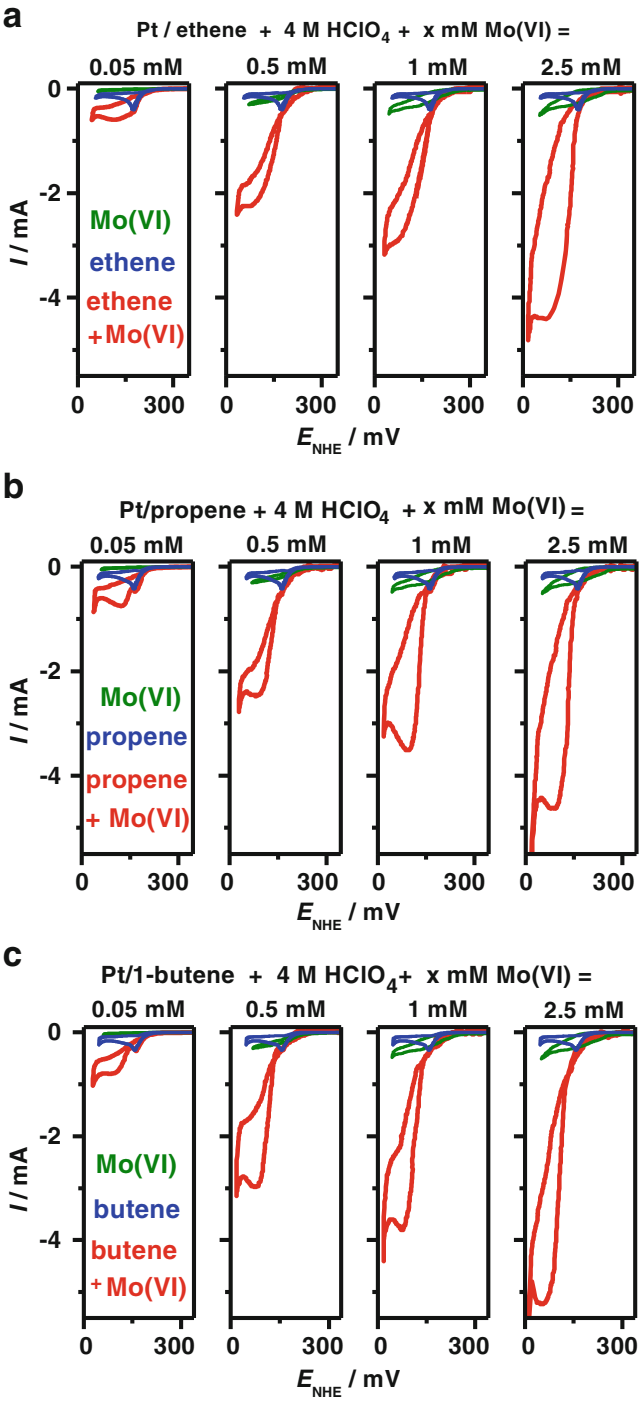

Fig. 5 Fragment of CVs on a polycrystalline Pt in 4-M $HClO_4$ solution with various $c_{Mo(VI)}$ for the electroreduction of **a** ethene, **b** propene and **c** 1-butene: *red lines,* third from the x-axis; alkene alone: *blue lines* second from the x-axis; Mo(VI) alone at the corresponding concentration: *olive lines* first from the x-axis. $v = 0.005$ V s^{-1}. (For interpretation of the references to colours in the figure legend, the reader is referred to the web version of this article)

the Pt electrode toward alkene hydrogenation when using 4-M $HClO_4$ as the supporting electrolyte (see also ref. [1]). This is manifested by the pronounced wave-shaped cathodic

peak current at E <0.25 V, with a maximum dependent on the $c_{Mo(VI)}$ value in the bulk of so strongly acidified solution containing a constant alkene concentration. On the contrary, no changes in the rate of alkene reduction were observed in the presence of molybdate in an acidic solution of pH >0, which contains solely dioxo- and trioxo- moieties of molybdic acid in equilibrium with Mo_{12}^{VI} to Mo_{36}^{VI} aggregates [15–17].

A comparison of CVs obtained for individual alkenes in the presence and absence of molybdate in 4-M $HClO_4$ solution with those characteristic of molybdate in the absence of alkene at the same pH value (see Fig. 5) leaves no doubt that the existence of cationic Mo(VI) oxo-species in the electrochemical cell is of primary importance for the appearance of the catalytic phenomenon in electroreduction of ethene, propene and 1-butene. This conclusion is corroborated by the absence of any increase in the current response corresponding to the alkene reduction on the Pt electrode modified with the electrochemically deposited mixed-valent Mo(VI)/Mo(V) layer and transferred into the alkene-saturated 4-M $HClO_4$ solution without Na_2MoO_4. By taking into account these results and our knowledge about the voltammetric behaviour of Mo(VI) oxo-species (Section 3.2), it is obvious that the magnitude of the reduction current observed in the alkene-Mo(VI) system strongly depends on the amount of cationic Mo(VI) species in the bulk solution.

The influence of increasing molybdate concentration and thus of an amount of cationic Mo(VI) species in 4-M $HClO_4$ solution on the reduction rate of ethene, propene and 1-butene on a Pt electrode is well illustrated in Fig. 5. As follows from the data collected in Fig. 6, there is a linear relation between the catalytic current at the potential of peak maximum (I_{pc}) and the molybdate concentration from $c_{Mo(VI)}$=0.05 mM to $c_{Mo(VI)}$=1 mM. Then I_{pc} approaches a limiting value at $c_{Mo(VI)}$≈2.5 mM, whereas the reduction rate of each alkene investigated is more than ten times greater in comparison with that in the absence of Mo(VI) and furthermore with that characteristic of the reduction of Mo(VI) alone. It is evident that this molybdate concentration in 4-M $HClO_4$ solution is optimal for efficient voltammetric detection of alkenes in real samples. Moreover, vice versa, an increased sensitivity of Mo(VI) detection can be achieved by introducing alkenes into the bulk solution.

It is noteworthy that the cathodic peak currents in CVs obtained for ethene, propene or 1-butene on the Pt electrode in 4-M $HClO_4$+ 2.5-mM Mo(VI) solution were almost independent of the scan rate up to v≈0.1 V/s, as predicted theoretically for the irreversible catalytic chemical reaction coupled to the preceding irreversible charge-transfer step [20–22]. This suggests that the

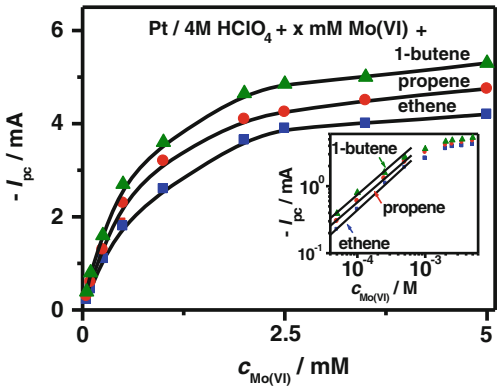

Fig. 6 Plot of the catalytic peak current corresponding to ethene, propene and 1-butene reduction on a polycrystalline Pt electrode in 4-M $HClO_4$ with Mo(VI) oxo-species, saturated with each alkene, vs concentration of Mo(VI) oxo-species in the bulk solution. *Insert* double logarithmic plot of the I_{pc} vs $c_{Mo(VI)}$ relationship presented in the main diagram. v= 0.005 V s^{-1}

catalytic effect, observed both in the alkenes and Mo(VI) reduction, results from continuous regeneration of the electroactive Mo(VI) and/or Mo(V) cationic oxo-species via a non-faradaic reaction between each individual alkene and the Mo(V) and/or Mo(III) moieties formed at the Pt/solution interface in the consecutive charge-transfer steps from the parent cationic Mo(VI) oxo-species. The appearance of cathodic current in CVs after reversal of the scan direction into positive one (see Fig. 5) supports this opinion. Unfortunately, it was not possible to establish the influence of the concentration of ethene, propene or 1-butene in the supporting electrolyte solution on the rate of their reduction. However, the shape of the respective I_{pc}-$c_{Mo(VI)}$ dependences presented for each of these compounds in Fig. 6 justifies the assumption that the reduction processes under study involves the formation of an associative adduct between the individual alkene and the cationic molybdenum species, due to interaction of π—electrons of the double bond of organics with unoccupied *ds* orbitals of molybdenum cations. One can expect that the presence of hydrogen in the structure of cationic Mo(V) and Mo(III) oxo-species (Section 3.2) facilitates the hydrogenation of alkene to alkane. The rate of the non-faradaic electron transfer from the conduction band of Mo(V) and/or Mo(III) species to the unsaturated organic species along with the addition of hydrogen to the C atoms at the double bond is most probably decisive for the overall reduction rate. The question is still open if alkenes form complexes with the reduced Mo(V) and/or Mo(III) cationic species only or also with the parent Mo(VI) cations.

Since the exact structure of molybdenum oxo-species taking part in the catalytic reduction of alkene at the Pt electrode is unknown at present, the reaction sequence

accounting for the enhancement of the reduction current in the alkene-Mo(VI) system investigated is proposed below for one of the possible protonated forms of such species.

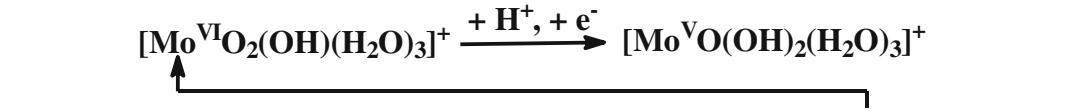

(3)

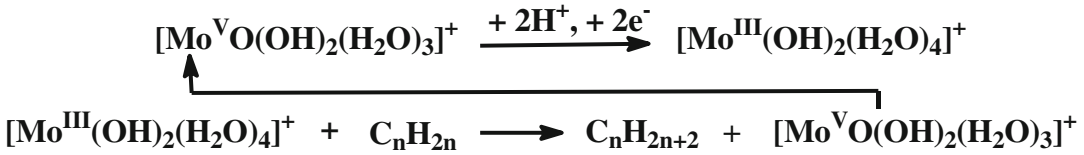

(4)

In the first pathway (3), the formation of alkane from alkene in the non-faradaic reaction with cationic Mo(V) moieties is accompanied by a continuous regeneration of the parent Mo(VI) species and their renewed electroreduction to Mo(V)species. The second pathway (4) involves electroreduction of the cationic Mo(V) species to the appropriate Mo(III) species, which in the non-faradaic reaction with alkene, giving alkane, are re-oxidised to the Mo(V) species and then re-reduced to Mo(III) moieties in the charge-transfer reaction at the Pt/solution interface. Keeping in mind that various cationic Mo(VI), Mo(V) and Mo(III) oxo-species may exists in solution, it cannot be excluded that all of them are involved in the catalysis.

Considering the experimental data exemplified in Fig. 5, it can be concluded that the pronounced catalytic effect of Mo(VI) in the ethene, propene and 1-butene reduction and vice versa appears in CVs at more negative electrode potentials than that of peak maximum obtained for these alkenes in a pure supporting electrolyte. This suggests that the electron transfer from Pt to cationic Mo(VI) oxo-species and the following non-faradaic reaction of Mo(V) and/or Mo(III) moieties with alkenes dissolved in solution near the electrode surface are preceded by the reductive desorption of alkene species pre-adsorbed on Pt at E >0.25 V, after the electroreduction of platinum oxide.

Further information about the mechanism and efficiency of the reduction processes in the Pt/alkene–molybdate–4-M $HClO_4$ system can be expected from studies with in situ spectroelectrochemical techniques. But even at present, the catalytic effect discovered in this system offers a possibility of a sensitive voltammetric detection of alkene and of Mo(VI) oxo-species.

Conclusions

Effective catalytic reduction of ethene, propene and 1-butene was demonstrated on a polycrystalline Pt electrode in a strongly acidic solution containing molybdate. The presence of cationic Mo(VI) oxo-species in the bulk solution proved to be essential for enhancement of the reduction current. This explains the influence of pH on the extent of catalysis. Simultaneously, the rate of electroreduction of cationic Mo(VI) oxo-species was appreciably increased in the presence of each alkene investigated. According to the experimentally established kinetic data, the observed catalytic phenomenon can be accounted for by the EC mechanism consisting in the continuous regeneration of the electroactive molybdenum species via a chemical reaction between alkene and the reduced cationic Mo(V) and/or Mo(III) moieties produced in the preceding charge-transfer steps at the Pt/solution interface. At the optimum molybdate concentration of 1–2.5 mM in 4-M $HClO_4$, the reduction rate of each individual alkene was found to be by about one order of magnitude greater as compared with that characteristic of the reduction of alkene or Mo(VI) species alone in the supporting electrolyte solution of the same concentration. Additional important finding is that Mo(VI) cations do not affect the behaviour of unsaturated organic compounds with triple C to C bond (ethyne, propyne) upon their reduction on Pt. Consequently, the Pt electrode in a strongly concentrated perchloric acid solutions appears to be attractive for practical application in a selective monitoring of alkene in the presence of Mo(VI) oxo-species and of Mo(VI) oxo-species in the presence of alkene in real samples.

Acknowledgments This work was supported by the Ministry of Science, Poland. The authors thank mgr Aleksandra Madaj for her technical assistance.

References

1. Bełtowska-Brzezinska M, Węsierski T, Łuczak T (2012) Electrochem Commun 24:5–8
2. Bełtowska-Brzezinska M, Łuczak T, Baltruschat H, Müller U (2003) J Phys Chem 107:4793–4800
3. Schmiemann U, Baltruschat H (1992) J Electroanal Chem 340:357–363
4. Baltruschat H, Schmiemann U (1993) Ber Bunsenges Phys Chem 97:452–460
5. Müller U, Schmiemann U, Dülberg A, Baltruschat H (1995) Surf Sci 335:33–342
6. Schmiemann U, Müller U, Baltruschat H (1995) Electrochim Acta 40:99–107
7. Baltruschat H (1999) Differential electrochemical mass spectrometry as a tool for interfacial studies. In: Wieckowski A (ed) Interfacial Electrochemistry. Marcel Dekker Inc, New York, Basel, pp 577–597
8. Löffler T, Bussar R, Xiao X, Ernst S, Baltruschat H (2009) J Electroanal Chem 629:1–14
9. Yoon C, Yang MX, Somorjai GA (1998) J Catal 176:35–41
10. Bełtowska-Brzezinska M, Łuczak T, Holze R (1998) Surf Sci 418:281–294
11. Bełtowska-Brzezinska M, Łuczak T, Holze R (1997) J Appl Electrochem 27:999–1011
12. Batina N, Chaffins SA, Gui JY, Lu F, McCargar JW, Rovang JW, Stern DA, Hubbard AT (1990) J Electroanal Chem 284:81–96
13. Bard AJ, Faulkner LR (2001) Electrochemical methods: fundamentals and applications, 2nd edn. Wiley, New York
14. Bełtowska-Brzezinska M, Węsierski T, Łuczak T, Camra J (2012) Electrochim Acta 63:89–99
15. Himeno S, Niiya H, Ueda T (1997) Bull Chem Soc Jpn 70:631–637
16. Cruywagen JJ, Heyns JBB (2000) Polyhedron 19:907–911
17. Ojo JF, Taylor RS, Sykes AG (1975) J Chem Soc Dalton Trans 500–505
18. a) Pope MT (1983) Heteropoly and isopoly oxometalates. Springer, Berlin, Heidelberg, New York, Tokyo, pp 1–180 b) Pope MT, Muller A (1991) Angew Chem Int Ed Eng 30:34–40
19. Taube F (2003) Characterization of aqueous peroxomolybdates with catalytic applicability http://www.diva-portal.org/umu/theses/marc21.xsql?dbid=45. Accessed 15 June 2005
20. Nicholson RS, Shain I (1964) Anal Chem 36:706–723
21. Galus Z (1994) Fundamentals of electrochemical analysis. Scientific Publisher, Warsaw
22. Polcyn DS, Shain I (1966) Anal Chem 38:376–382